Traditional analysis of aquifer tests: Comparing apples to oranges?

Cheng-Mau Wu,[1] Tian-Chyi J. Yeh,[2] Junfeng Zhu,[2] Tim Hau Lee,[1] Nien-Sheng Hsu,[1] Chu-Hui Chen,[3] and Albert Folch Sancho[4]

Received 6 October 2004; revised 19 May 2005; accepted 3 June 2005; published 2 September 2005.

[1] Traditional analysis of aquifer tests uses the observed drawdown at one well, induced by pumping at another well, for estimating the transmissivity (*T*) and storage coefficient (*S*) of an aquifer. The analysis relies on Theis' solution or Jacob's approximate solution, which assumes aquifer homogeneity. Aquifers are inherently heterogeneous at different scales. If the observation well is screened in a low-permeability zone while the pumping well is located in a high-permeability zone, the resulting situation contradicts the homogeneity assumption in the traditional analysis. As a result, what does the traditional interpretation of the aquifer test tell us? Using numerical experiments and a first-order correlation analysis, we investigate this question. Results of the investigation suggest that the effective *T* and *S* for an equivalent homogeneous aquifer of Gaussian random *T* and *S* fields vary with time as well as the principal directions of the effective *T*. The effective *T* and S converge to the geometric and arithmetic means, respectively, at large times. Analysis of the estimated *T* and *S*, using drawdown from a single observation well, shows that at early time both estimates vary with time. The estimated *S* stabilizes rapidly to the value dominated by the storage coefficient heterogeneity in between the pumping and the observation wells. At late time the estimated *T* approaches but does not equal the effective *T*. It represents an average value over the cone of depression but influenced by the location, size, and degree of heterogeneity as the cone of depression evolves.

Citation: Wu, C.-M., T.-C. J. Yeh, J. Zhu, T. H. Lee, N.-S. Hsu, C.-H. Chen, and A. F. Sancho (2005), Traditional analysis of aquifer tests: Comparing apples to oranges?, *Water Resour. Res.*, *41*, W09402, doi:10.1029/2004WR003717.

1. Introduction

[2] The transmissivity (*T*) and storage coefficient (*S*) are two important properties that control groundwater flow in aquifers and are of practical importance for water resources development and management. Traditionally, these aquifer properties are determined by collecting drawdown time data of the aquifer induced by pumping, and then matching the data with analytical solutions, which assume homogeneity of the aquifer. Theis' solution [*Theis*, 1935] is one of the commonly used analytical solutions in aquifer tests. It is derived from the equation of unsteady radial, horizontal, groundwater flow in a confined aquifer with constant *T* and *S*. Although the Theis solution is strictly applicable only to such idealized flow and aquifer conditions, it has been widely used in the field to estimate aquifer properties given drawdown time data from an observation well during an aquifer test.

[3] Radial flow in heterogeneous aquifers has been studied by many researchers in the past [see *Meier et al.*, 1998]. In particular, *Butler and Liu* [1993] derived an analytical solution for the case of transient, pumping-induced drawdown in a uniform aquifer into which a disk-shaped inclusion of anomalous properties (different *T* and *S*) has been placed. They found that changes in drawdown are sensitive to the hydraulic properties of a discrete portion of an aquifer for a time of limited duration. After that time, it is virtually impossible to gain further information about those properties. They concluded that constant rate pumping tests are not an effective tool for characterizing lateral variation in flow properties. *Oliver* [1993] derived the Fréchet derivatives and kernels to study the effect of areal variations in *T* and *S* on drawdown at an observation well. He concluded that small-scale variation in *T* near the well bore can influence the late time drawdown at distant observations depending on the location of the nonuniformity. Interpretation of a drawdown anomaly might be difficult because the effect on the drawdown derivative of a spatially small near-well nonuniformity is similar to the effect of a spatially large nonuniformity located farther from the well bore. *Meier et al.* [1998] conducted numerical simulations of pumping tests in two-dimensional horizontal aquifers with spatially varying *T* and a constant *S*. Analyzing the simulated drawdown at observation wells at various distances from the pumping well, they found that the estimated *T* from late time drawdown data using the Cooper-Jacob method [*Cooper and Jacob*, 1946] is very close to the effective *T* of the medium for uniform flows, practically independent of the location of the observation point. *Sánchez-Vila et al.* [1999] conducted an analytical study of drawdown under flow toward a well in heterogeneous

[1]Department of Civil Engineering, National Taiwan University, Taipei, Taiwan.
[2]Department of Hydrology and Water Resources, University of Arizona, Tucson, Arizona, USA.
[3]Department of Civil Engineering, ChungKuo Institute of Technology, Taipei, Taiwan.
[4]Unitat de Geodinàmica Externa i Hidrogeologia, Departamento de Geologia, Universitat Autònoma de Barcelona, Bellaterra, Spain.

Copyright 2005 by the American Geophysical Union.
0043-1397/05/2004WR003717$09.00

aquifers of spatially varying T with a constant S. Using Jacob's method, they showed that estimated T values for different observation points tend to converge to the effective T derived under parallel flow conditions. Estimated S values, however, displayed higher variability but the geometric mean of the estimated S values could be used as an unbiased estimator of the actual S.

[4] Using an analytical stochastic approach, *Indelman* [2003] investigated the unsteady well flow in heterogeneous aquifers by modeling the hydraulic conductivity (K) as a three-dimensional stationary random function of axisymmetric anisotropy and Gaussian correlations. He assumed that the aquifer thickness is uniform and much greater than the vertical correlation scale of K, and specific storage S_s is a deterministic constant. Then, closed-form approximations of the ensemble mean drawdown were derived. He showed that the T estimated based on the ensemble mean drawdown, using the Cooper-Jacob asymptotic, is precisely the effective conductivity for uniform horizontal flow.

[5] These studies in general have suggested that the conventional Cooper-Jacob method is viable for estimating mean parameter values in heterogeneous aquifer from late time data, or a long duration of pumping. These studies, however, have not investigated effects of the variability of S on the T and S estimates, nor do they examine the behaviors of T and S estimates at early times. The behaviors of T and S estimates at early times can be important because an extended pumping could include effects of large-scale heterogeneity, as well as boundary effects. More importantly, few studies have examined the meaning of estimated S for heterogeneous aquifers. Even if they have, they have assumed that aquifers are made of spatially variable T and a spatially uniform S. Since the storage coefficient is the key parameter for evaluating groundwater availability in a basin, knowing the real meanings of the estimate of S in aquifers with heterogeneous S is of critical importance to groundwater resource management.

[6] Therefore previous numerical and theoretical analyses are incomplete. A practical but important question remains: What kind of estimates of the properties do we obtain from either early or late time drawdown data from an individual observation well in a heterogeneous aquifer? Also, do the estimates reflect the local properties near the observation well, some averaged properties between the pumping well and observation well, or none of the above?

[7] To answer these questions, this paper develops two theoretically consistent methods (i.e., distance drawdown and spatial moments) to estimate the effective transmissivity (T_{eff}) and storage coefficient (S_{eff}) values for radial flow in a given aquifer, as opposed to an ensemble of aquifers. Using numerical simulations and cross-correlation analysis, we investigate effects of heterogeneity in both T and S on the analysis of traditional aquifer tests using the Theis analytic solution.

2. Effective Parameters of Heterogeneous Aquifer

[8] Consider a two-dimensional (2-D) flow equation with horizontally varying transmissivity, T, and storage coefficient, S:

$$\nabla \cdot (T \nabla h) = S \frac{\partial h}{\partial t} \tag{1}$$

where $h(x_i, t)$ is the hydraulic head, x_i (where $i = 1, 2$) and t are spatial coordinates and time, respectively. The head, h, is the depth-averaged head, equivalent to the head observed in a fully penetrating and screened well. We choose the 2-D depth integrated model because the variability in T and S includes not only the multiscale heterogeneous nature of the aquifer hydraulic properties but also the variation in thickness of the aquifer, which is difficult to implement in a 3-D analysis.

[9] If both T and S are conceptualized as spatial stochastic processes, equation (1) then can be written as

$$\nabla \cdot \left[\left(\overline{T} + T' \right) \nabla \left(\overline{h} + h' \right) \right] = \left(\overline{S} + S' \right) \frac{\partial \left(\overline{h} + h' \right)}{\partial t} \tag{2}$$

where the overhead bar and prime represent mean and perturbation of the variable, respectively. Taking the expected value (ensemble average) of equation (2) leads to

$$\nabla \cdot \left[\overline{T} \nabla \overline{h} \right] + E \langle \nabla \cdot [T' \nabla h'] \rangle = \overline{S} \frac{\partial \overline{h}}{\partial t} + E \left\langle S' \frac{\partial h'}{\partial t} \right\rangle \tag{3}$$

If the second term on the left-hand side of equation (3) is assumed to be proportional to the mean hydraulic gradient, the left-hand side then can be expressed as

$$\begin{aligned} \nabla \cdot \left[\overline{T} \nabla \overline{h} \right] + \nabla \cdot E \langle T' \nabla h' \rangle &= \nabla \cdot \left[\left(\overline{T} + E \left\langle T' \nabla h' \right\rangle \left[\nabla \overline{h} \right]^{-1} \right) \nabla \overline{h} \right] \\ &= \nabla \cdot \left[T_{eff} \nabla \overline{h} \right] \end{aligned} \tag{4}$$

where $T_{eff} = \overline{T} + E \langle T' \nabla h' \rangle \left[\nabla \overline{h} \right]^{-1}$ is the effective transmissivity of the heterogeneous aquifer. Similarly, assuming the second term on the right-hand side is proportional to the change in mean hydraulic head, the right-hand side can be expressed as

$$\overline{S} \frac{\partial \overline{h}}{\partial t} + E \left\langle S' \frac{\partial h'}{\partial t} \right\rangle = \left(\overline{S} + E \left\langle S' \frac{\partial h'}{\partial t} \right\rangle \left(\frac{\partial \overline{h}}{\partial t} \right)^{-1} \right) \frac{\partial \overline{h}}{\partial t} = S_{eff} \frac{\partial \overline{h}}{\partial t} \tag{5}$$

where $S_{eff} = \overline{S} + E \langle S' \frac{\partial h'}{\partial t} \rangle / \frac{\partial \overline{h}}{\partial t}$ is the effective storage coefficient of the aquifer. Using equations (4) and (5), the ensemble mean flow equation for the heterogeneous aquifer takes the following form:

$$T_{eff} \nabla^2 \overline{h} = S_{eff} \frac{\partial \overline{h}}{\partial t} \tag{6}$$

in which T_{eff} and S_{eff} are ensemble effective hydraulic properties, which become spatially constant after an excitation has propagated for a period of time (analogous to *Talyor*'s [1921] analysis of diffusion). The spatially constant properties are attributed to the highly diffusive nature of the head process. In equation (6), $\overline{h}$ is the ensemble mean head for the 2-D heterogeneous aquifer.

[10] In order to apply equation (6) to a heterogeneous aquifer (one single realization of the ensemble), the aquifer can be conceptualized as an equivalent homogeneous medium either in the ensemble mean or in the spatial

average sense. In the ensemble sense, the T_{eff} and S_{eff} ensemble effective parameters with equation (6) yields the ensemble mean head, $\overline{h}$, which represents the average head of many realizations of possible heterogeneous aquifers. The mean head will equal the spatially averaged head in a heterogeneous aquifer (one realization) if ergodicity exists. In other words, the two heads will be equivalent if the area that defines the spatial average head encompasses most of the heterogeneity in the aquifer. This area in general must be many times the correlation scale of the heterogeneity. Under the ergodic condition, the heterogeneous aquifer can be treated as a spatially homogeneous medium with uniform T_{eff} and S_{eff} (i.e., effective parameters for the equivalent homogeneous aquifer). These properties are similar to (but not equal to) those defined in an REV (representative elementary volume) for homogeneous media in the classical groundwater hydrology. The REV is defined as a control volume, or control volumes, whose volume-averaged hydraulic properties are representative of every part of the field medium regardless of the location of the control volume in the medium [*Bear*, 1988; *de Marsily*, 1986].

[11] As discussed above, equation (6) is valid for a single realization if the ergodicity of head exists in the field. However, an observed head at a well in a heterogeneous aquifer merely represents a point measurement (i.e., apples), which is different from the spatially averaged head (i.e., oranges) that satisfies the ergodicity assumption embedded in equation (6). Despite this inconsistency, hydrologists have frequently used the Theis solution, built upon equation (6), to estimate effective aquifer parameters of a heterogeneous aquifer using the drawdown at an observation well. So, are we comparing apples to oranges?

2.1. Traditional Analysis of Aquifer Tests

[12] Suppose that the head observed in a well is indeed equivalent to the head ($\overline{h}$) in equation (6). The solution of equation (6) with auxiliary conditions in terms of drawdown caused by pumping at a well is [*Theis*, 1935]

$$\overline{s} = \frac{Q}{4\pi T_{eff}} W(u); \quad u = \frac{S_{eff} r^2}{4 T_{eff} t}, \quad W(u) = \int_u^{\infty} \frac{e^{-x}}{x} dx. \tag{7}$$

where $\overline{s}(r, t) = \overline{h}(r, t) - \overline{h}_0(r, t)$, $\overline{h}_0$ is the head before pumping, and $\overline{s}(r, t)$ is the drawdown at time t and a radial distance r from the pumping well.

[13] To estimate T_{eff} and S_{eff} parameters, a nonlinear least squares minimization approach is often applied to minimizing the following objective function

$$\sum_{j=1}^{n} \left[\overline{s}(r, t_j) - s^*(r, t_j)\right]^2 \tag{8}$$

where $\overline{s}(r, t)$ and $s^*(r, t)$ are the theoretical drawdown in an equivalent homogeneous aquifer predicted by equation (7), and the observed drawdown at a distance r from the pumping well in an aquifer at time t_j, respectively; j is an index of the observation time; n is the total number of observation times. Since the observed head may not satisfy the ergodicity assumption, the validity of using traditional analysis for estimating T_{eff} and S_{eff} parameters becomes the question. We will thus distinguish the estimated T and S based on the traditional analysis using the symbols, $\hat{T}$ and $\hat{S}$, from the effective properties, T_{eff} and S_{eff}.

2.2. Drawdown Distance Analysis

[14] In accordance with the aforementioned effective property theory, if the drawdown is a point measurement in a heterogeneous aquifer, it is then necessary to fit equation (7) to the drawdown data everywhere in the aquifer so that values of T_{eff} and S_{eff}, consistent with the theory of Theis, can be sought. That is, one should seek the parameter values to minimize the following objective function:

$$\sum_i \left[\overline{s}(r_i, t) - s^*(r_i, t)\right]^2 \tag{9}$$

where $\overline{s}(r_i, t)$ and $s^*(r_i, t)$ are the theoretical drawdown in an equivalent homogeneous aquifer predicted by equation (7) and the observed drawdown at an observation well at a distance r_i from the pumping well in an aquifer at a given time t, respectively. The sum of the difference squared is applied at every point, i, in the aquifer at a given time. If T_{eff} and S_{eff} values are spatially uniform parameters, then their estimates based on equation (9) should be time invariant. This is a correct approach for defining the effective parameters for an equivalent homogeneous formation as demonstrated by *Bosch and Yeh* [1989] and *Yeh* [1989] for effective hydraulic properties for unsaturated porous media. Therefore correct effective hydraulic properties used in the flow equation that assumes homogeneity should only yield unbiased predictions of overall (mean) system responses, but not their details. In fact, this is the approach commonly called drawdown distance analysis in the analysis of aquifer tests [*Walton*, 1970]. This approach has, in practice, rarely been used because of the number of observation wells is typically limited. Nevertheless, this approach is possible in this study because numerical experiments are employed in which drawdown everywhere in a simulation domain is known. Thus equation (9) is used to derive the theoretically correct T_{eff} and S_{eff} values.

2.3. Spatial Moment Analysis of the Drawdown Distributions

[15] Parallel to the drawdown distance analysis, we here introduce a spatial moment approach to determine the T_{eff} and S_{eff} values. To quantify the spread of the drawdown at different times, the spatial moments [*Aris*, 1956] can be used:

$$M_{ij}(t) = \int_{-\infty}^{+\infty} \int_{-\infty}^{+\infty} s(x, y, t) x^i y^j dx dy \tag{10}$$

where $s(x, y, t)$ represents the drawdown at a given time t at a location x and y. The zeroth, first, and second spatial moments correspond to $i + j = 0$, 1, and 2, respectively. The zeroth moment (M_{00}) represents the change in volume of the cone of depression (i.e., drawdown) caused by pumping. The center of mass location (x_c, y_c) of the cone of depression (the location of the pumping well) at a given time is represented by

$$x_c = M_{10}/M_{00} \quad \text{and} \quad y_c = M_{01}/M_{00} \tag{11}$$

The spread of the cone about its center is described by the symmetric second spatial variance tensor:

$$\sigma^2 = \begin{bmatrix} \sigma_{xx}^2 & \sigma_{xy}^2 \\ \sigma_{yx}^2 & \sigma_{yy}^2 \end{bmatrix} \quad \sigma_{xx}^2 = \frac{M_{20}}{M_{00}} - x_c^2 \qquad \sigma_{yy}^2 = \frac{M_{02}}{M_{00}} - y_c^2 \qquad (12)$$
$$\sigma_{xy}^2 = \sigma_{yx}^2 = \frac{M_{11}}{M_{00}} - x_c y_c$$

Ye et al. [2005] applied this moment approach to snapshots of moisture plumes to study moisture plume dynamics at the Hanford site, Washington.

[16] Suppose T_{eff} and S_{eff} values are spatial constants as in equation (6), the equation then can be rewritten as a diffusion equation with a constant diffusivity, $D_{eff} = T_{eff}/S_{eff}$:

$$D_{eff} \nabla^2 \overline{h} = \frac{\partial \overline{h}}{\partial t} \qquad (13)$$

This equation is identical to the diffusion equation for solutes. Following *Fisher et al.* [1979], the diffusivity tensor can be related to the rate of change in the second spatial moments of the drawdown distribution induced by pumping:

$$D_{eff}^{xx} = \frac{1}{2}\frac{\partial \sigma_{xx}^2}{\partial t}, \; D_{eff}^{yy} = \frac{1}{2}\frac{\partial \sigma_{yy}^2}{\partial t}, \text{ and } D_{eff}^{xy} = D_{eff}^{yx} = \frac{1}{2}\frac{\partial \sigma_{xy}^2}{\partial t} \qquad (14)$$

where D_{eff}^{xx} and D_{eff}^{yy} are the diagonal components and D_{eff}^{xy} and D_{eff}^{yx} are the off-diagonal components of the effective diffusivity tensor.

[17] Then S_{eff} is the ratio of the pumping rate, Q, to the rate of change in the zeroth moment, assuming that flow contributing to the Q is entirely from the cone of depression. Next, according to equation (14) and the estimated S_{eff}, the effective transmissivity tensor components thus can be calculated and the anisotropy in effective transmissivity can be determined. *Yeh et al.* [2005] applied a similar approach to determining the 3-D effective unsaturated hydraulic conductivity tensor using snapshots of a moisture plume in the vadose zone at the Hanford field site in Richland, Washington.

2.4. First-Order Cross-Correlation Analysis

[18] To gain insight of the meaning of the $\hat{T}$ and $\hat{S}$ obtained from the traditional aquifer test and analysis, a first-order cross-correlation analysis is carried out. The purpose of this analysis is to show the relation between the head behavior at an observation well with T and S values anywhere of an aquifer during flow induced by a pumping well.

[19] Expanding the hydraulic head at a location in equation (1) in a Taylor series about the mean values of parameters, and neglecting second- and higher-order terms, the head perturbation at location i at a given time t can be expressed as

$$h_i' = T_j' \frac{\partial h_i}{\partial T_j}\Big|_{T,S} + S_j' \frac{\partial h_i}{\partial S_j}\Big|_{T,S} = \mathbf{T}'\mathbf{J}_{hT} + \mathbf{S}'\mathbf{J}_{hS} \qquad (15)$$

where T_j' and S_j' are perturbation of T and S at location j and j = 1, . . .N, which is the total number of elements in the domain; $\frac{\partial h_i}{\partial T_j}$ and $\frac{\partial h_i}{\partial S_j}$ are the sensitivity of h at location i at a given time t with respect to T and S perturbation at location j. The sensitivity terms in equation (4) are calculated by the adjoint state method [*Sykes et al.*, 1985; *Li and Yeh*, 1998; *Zhu and Yeh*, 2005]. Assuming T and S are mutually independent from each other, the covariance of h', the cross covariance of h' and T' and the cross covariance of h' and S' can be expressed [see *Hughson and Yeh*, 2000], respectively, as

$$\begin{aligned} \mathbf{R}_{hh}(\mathbf{x}_i, \mathbf{x}_j, t) &= \mathbf{J}_{hT}\mathbf{R}_{TT}(\mathbf{x}_i, \mathbf{x}_j)\mathbf{J}_{hT}^T + \mathbf{J}_{hS}\mathbf{R}_{SS}(\mathbf{x}_i, \mathbf{x}_j)\mathbf{J}_{hS}^T \\ \mathbf{R}_{hT}(\mathbf{x}_i, \mathbf{x}_j, t) &= \mathbf{J}_{hT}\mathbf{R}_{TT}(\mathbf{x}_i, \mathbf{x}_j) \\ \mathbf{R}_{hS}(\mathbf{x}_i, \mathbf{x}_j, t) &= \mathbf{J}_{hS}\mathbf{R}_{SS}(\mathbf{x}_i, \mathbf{x}_j) \end{aligned} \qquad (16)$$

The cross covariances, $\mathbf{R}_{hT}$ and $\mathbf{R}_{hS}$, are then normalized by the square root of the product of the variances of h at t and T or those of h at t and S to obtain their corresponding cross correlation at locations i and j at time t. The cross correlation represents how the head perturbation at location i at a given time is influenced by the T or S perturbation at location j. With a given mean T, S and a pumping rate, these cross covariances are evaluated numerically using the algorithm in the hydraulic tomography inverse model developed by *Zhu and Yeh* [2005] based on an earlier work by *Hughson and Yeh* [2000]. While it is similar to the perturbation analysis by *Oliver* [1993], the cross-correlation analysis is numerical and includes correlation structures of T and S.

3. Numerical Experiments and Analysis

[20] The procedure for the numerical experiment consists of the following steps: (1) generating one realization of 2-D heterogeneous T and S fields (they are perfectly correlated with each other), (2) simulating flow to a well in this realization, using variably saturated flow and transport in two dimensions (VSAFT2) [*Yeh et al.*, 1993], (3) conducting the drawdown distance and spatial moment analyses to determine the T_{eff} and S_{eff} of the realization, (4) obtaining $\hat{T}$ and $\hat{S}$ using the traditional approach based on the drawdown time data from individual observation wells in this aquifer, and (5) geometrically and arithmetically averaging the values of T and S of each finite element within the cone of depression during pumping to derive T_{Gave} and S_{Gave}, and T_{Aave} and S_{Aave}, respectively, and comparing these averages with T_{eff} and S_{eff}, and $\hat{T}$ and $\hat{S}$.

[21] The synthetic heterogeneous aquifer is square in shape, and is discretized into 50 × 50 square elements and bounded by constant head boundary conditions. Each element is 40 cm in length. The pumping well is located at the center of the simulated field. The observation wells are assigned in four radial directions for determining $\hat{T}$ and $\hat{S}$. Figure 1 shows the layout of the numerical experiment and the locations of the wells.

[22] The synthetic T and S fields, which have similar properties to the study of *Jonse et al.* [1992], were generated on the 40 cm × 40 cm grid, using a Gaussian random field generator by *Gutjahr* [1989]. The geometric mean value of T is given as 0.00184 cm^2/s (arithmetic mean = 0.00844). The value of LnT variance ($\sigma_{\ln T}^2$) considered in this analysis is 3.25. The geometric mean of S is given as 0.0014 (arithmetic mean = 0.00865), and the value of LnS variance ($\sigma_{\ln S}^2$) is 3.93. The correlation scale is 80 cm in both x and y directions. The spatial distribution of the generated T field is

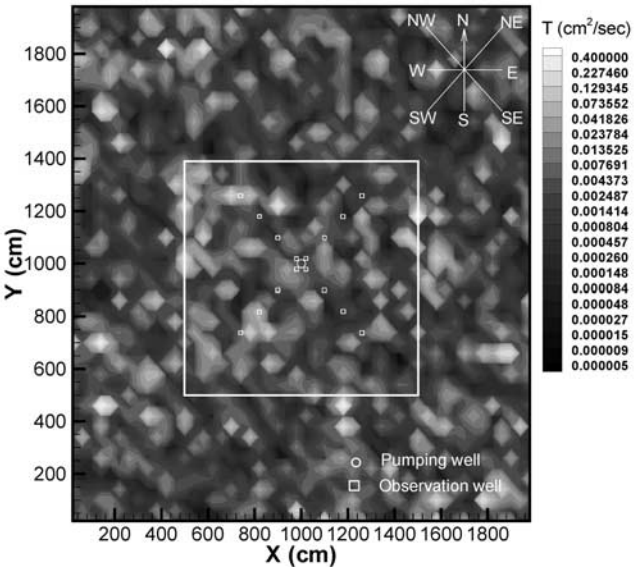

Figure 1. Illustration of the synthetic heterogeneous T (cm^2/s) field used in the analysis.

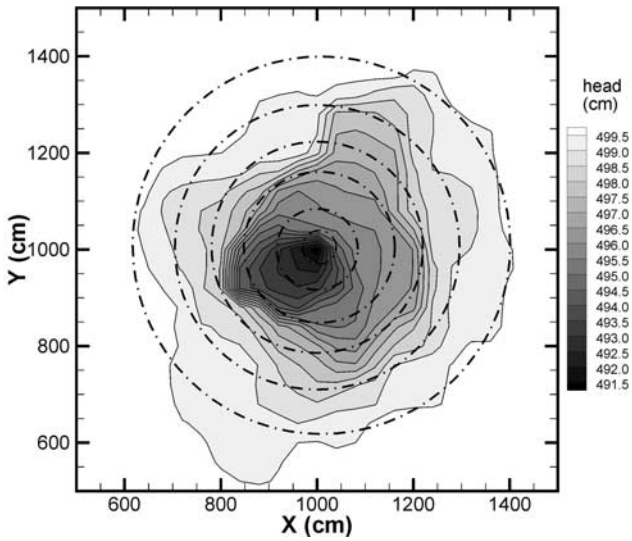

Figure 2. Head distribution in the heterogeneous and equivalent homogeneous aquifers after one pumping for 24 hours.

illustrated in Figure 1. The spatial distribution of S has the same variation pattern as the T field. The pumping rate is a constant, 1 cm^3/s. The small mean T value is used to avoid rapid propagation of the cone of the depression to the boundary. The large variances are used to underscore the questions we raised earlier.

3.1. Effective Properties, T_{eff} and S_{eff}, of Heterogeneous Media

[23] Figure 2 shows the contour of highly irregular head distribution after pumping for one day in the synthetic heterogeneous aquifer. The concentric circles indicated by the dash-dotted lines indicate the head distribution in an equivalent homogeneous aquifer with the estimated T_{eff} and S_{eff} derived from the distant drawdown analysis (discussed later in this section). Figure 2 demonstrates that the effective parameters do not reproduce the exact drawdown distribution in a heterogeneous aquifer, but only the overall drawdown behavior in the aquifer. This leads to the salient question that we posed earlier: If the drawdown in a heterogeneous aquifer cannot be predicted by the Theis approach, why do we force the Theis solution to match the drawdown observed at a point in a heterogeneous aquifer to derive the effective hydraulic properties of the aquifer? Are we comparing apples to oranges? If so, what do the estimates mean?

[24] As discussed in section 2.2., the drawdown distance analysis is consistent with the equivalent homogeneous aquifer concept embedded in Theis' solution. On the basis of this premise we apply equation (9) to the simulated head values at every node of the synthetic aquifer to derive T_{eff} and S_{eff}. Figure 3 shows the estimated T_{eff} values (normalized by the geometric mean of the entire domain) as a function of pumping time. As postulated by *Yeh* [1998] on the basis of a diffusion concept [*Taylor*, 1921], the value of T_{eff} varies with time. Its value is greater than the geometric mean (0.00184) of the entire aquifer at early time, then approaches and equals the geometric mean at large time.

[25] The normalized S_{eff} values (the estimates divided by the geometric mean of S values, 0.0014, in the aquifer) in Figure 4 show that S_{eff} varies with time and approaches the arithmetic mean (0.00865) of the field at large time. This can be attributed to the fact that the effective storage coefficient is not affected by flow (see section 3.4, discussion of Figure 9b). This finding agrees with the result of the analysis by *Chrysikopoulos* [1995] in which the effective specific storage is reported to equal its volume average.

[26] Besides the drawdown distance analysis, we calculated the T_{Gave} and S_{Gave} values using geometrical averages of values of T and S, as well as the arithmetic average of T and S values (i.e., T_{Aave} and S_{Aave}, respectively) of each element within the cone of depression. The cone of depres-

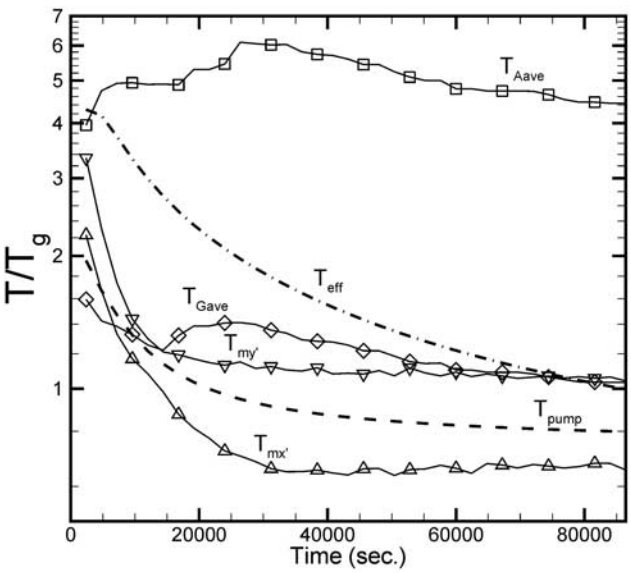

Figure 3. Effective transmissivity, T_{eff}, geometrically and arithmetically averaged transmissivity, T_{Gave} and T_{Aave}, over the cone of depression, $T_{mx'}$ and $T_{my'}$, in the principal directions, estimated using the moment approach, and transmissivity estimated from the pumping well, T_{pump}. Notice a log scale is used for the vertical axis.

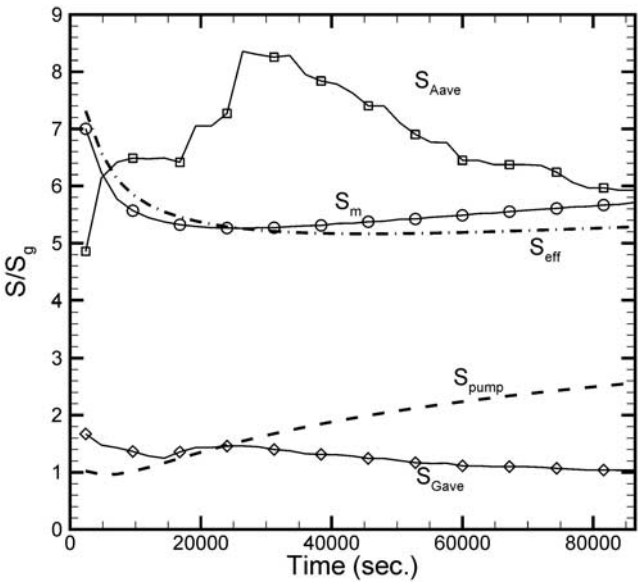

Figure 4. Effective storage coefficient, S_{eff}, geometrically and arithmetically averaged storage coefficients, S_{Gave} and S_{Aave}, over the cone of depression, and storage coefficient estimated from the pumping well, T_{pump}.

sion is defined as the area where drawdown is greater than zero. The number of T and S values included in the average increases as the cone of depression expands. Normalized T_{Gave} and, T_{Aave} values are shown as diamonds and squares, respectively, in Figure 3 as a function of time. Figure 4 shows the evolution of S_{Gave} and, S_{Aave} (diamond and square, respectively). While both T_{Gave} and S_{Aave} values are different from T_{eff} and S_{eff} at early time, they agree with T_{eff} and S_{eff} at large time. The S_{Aave} value however takes a longer time to approach S_{eff} than the T_{Gave} value. Furthermore, the S_{Aave} values are much closer to S_{eff} at all times than the S_{Gave} values.

[27] These results suggest that: 1) an REV exists when the area of averaging is much greater than many times the correlation scale of the heterogeneity; and 2) at early time the flow is nonergodic and cannot be described by equation (6). Only at large time does the flow becomes ergodic, equation (6) becomes valid, and the T_{eff} and S_{eff} values based on equation (6) coincide with those of the REV (see section 2).

[28] The second spatial moments of the simulated drawdown at different time in the heterogeneous aquifer are plotted in Figure 5. The spatial variances in x and y directions are different, and initially increase nonlinearly with time and then linearly after time is greater than 20,000 s. The xy component of the spatial variance tensor decreases from zero and then increases and becomes greater than zero. These results suggest that the overall shape of the cone of depression is slightly elliptic and its principal directions vary with time. On the basis of the slopes of the linear portions of the spatial variances and equation (14) we found that D_{eff} in the x, y, and xy directions are 0.2278, 0.1917, and 0.04695 cm^2/s, respectively. After coordinate transformation, the D_{eff} in the principal directions, x' and y', are 0.260 and 0.159 cm^2/s, respectively, indicative of anisotropy in the effective diffusivity. This anisotropy is a manifestation of the effect of local heterogeneity even though the medium is statistically isotropic. The plot of $T_{x'}$ and $T_{y'}$ are shown in Figure 3 and the estimated S based on the spatial moment method is shown in Figure 4. This result agrees with the values of T_{eff} and S_{eff} found by our drawdown distance analysis, which assumes isotropic effective properties. Likewise, the nonlinear behavior of the second spatial moments, concurring with the results of the drawdown distance analysis, is indicative of the nonexistence of an REV and nonergodic head fields (i.e., the effective properties vary with time during the early stage of the pumping test).

3.2. Estimation of $\hat{T}$ and $\hat{S}$ From the Pumping Well

[29] A common practice in aquifer tests is to estimate parameters from the drawdown time data obtained from the pumping well. Figure 3 shows that when the pumping time is sufficiently long, the $\hat{T}$ estimated using the drawdown at the pumping well approaches T_{eff}, but is lower than T_{eff}. Conversely, the estimated $\hat{S}$ at the pumping well shows greater deviation from S_{eff} than $\hat{T}$ (see Figure 4).

3.3. Estimates Based on the Drawdown From a Single Observation Well

[30] In the following analysis, observation wells are assigned at different radii (28.28, 84.85, 141.42, and 197.99 cm) in four directions: NE, SE, SW, and NW (Figure 1). Well drawdown time data from these wells are analyzed using the traditional drawdown time analysis (equation 8) to obtain $\hat{T}$ and $\hat{S}$ values.

[31] The normalized $\hat{T}$ values (the estimate divided by the geometric mean of the T field) from drawdown of four wells at radius r = 84.85 cm are shown in Figure 6. Unfilled circle, diamond, triangle, and square symbols denote the estimates from the wells in the NE, SE, SW, and NW directions, respectively. The dash-dotted line in the Figure 6 denotes T_{eff}. According to Figure 6, the $\hat{T}$ values estimated from individual observation wells evolve with time. At early time, each well yields dramatically different estimates. They eventually approach the T_{eff} value at large time but are smaller and bear the same high and low orders of the $\hat{T}$ values as those at early time. Although not shown here, $\hat{T}$

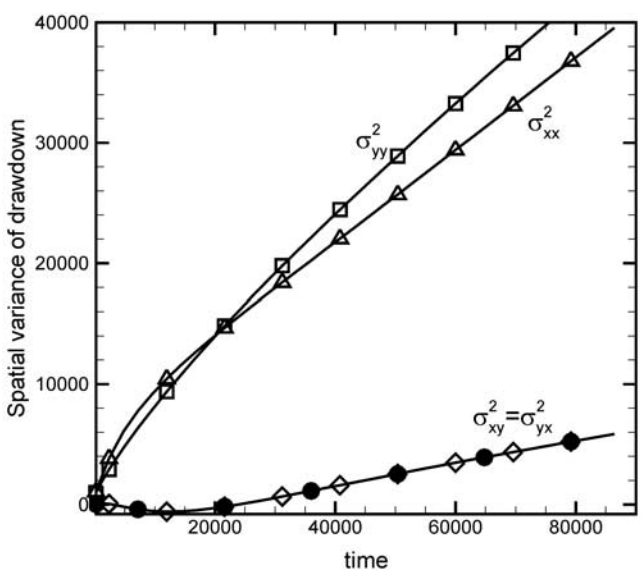

Figure 5. Spatial variances of the drawdown.

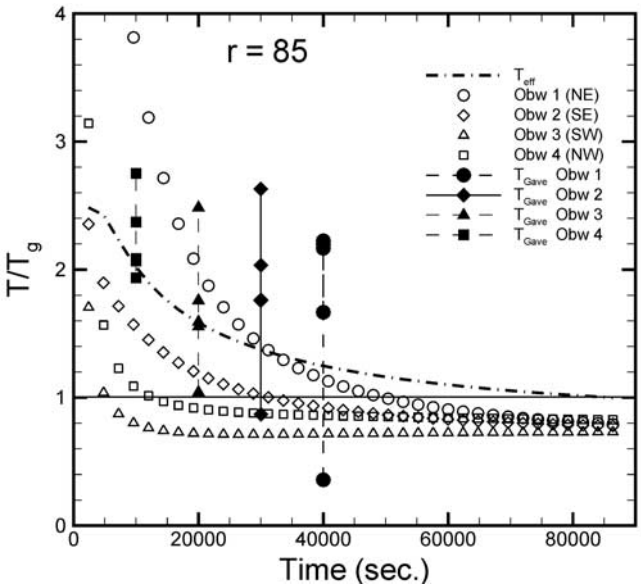

Figure 6. Estimated transmissivity values, $\hat{T}$, from different observation wells at a radial distance of 84.85 cm and averaged T over four areas around the wells.

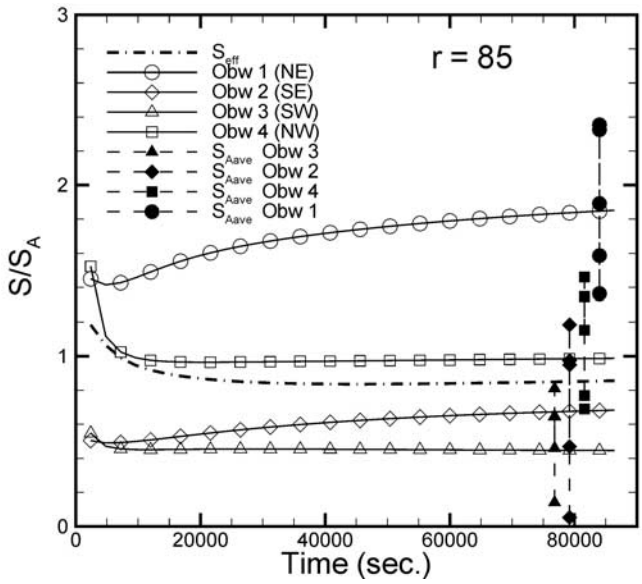

Figure 7. Estimated storage coefficient values, $\hat{S}$, from different observation wells at a radial distance of 84.85 cm and averaged S over four different areas around the wells.

values from observation wells located at a greater radius have similar behaviors as in Figure 6. However, they exhibit greater variability than those in Figure 6 at early times, and take longer to approach the T_{eff} value. This finding is consistent with that of *Meier et al.* [1998] and *Sánchez-Vila et al.* [1999] in that the values of $\hat{T}$ estimated from different wells tend to be fairly constant.

[32] In Figure 6, solid circles, diamonds, triangles, and squares (connected by vertical lines) denote locally averaged T values around the observation wells in NE, SE, SW, and NW direction, respectively. Five different averages are shown for each well; they represent the geometrically averaged T values over 4, 16, 36, 64, or 100 elements surrounding the well. As illustrated, $\hat{T}$ values based on the early time observed drawdown at each well do not necessarily correlate with the locally averaged T values. At large time, the stabilized $\hat{T}$ values maintain their high/low orders and do not corroborate well with the locally averaged transmissivity values (see section 3.5 for explanation).

[33] Figure 7 shows the normalized $\hat{S}$ values (i.e., the values divided by the arithmetic mean of the S field) based on the drawdown from the wells in the four directions at r = 84.85 cm. Overall, high variability is found for $\hat{S}$ as reported by *Sánchez-Vila et al.* [1999] although they assumed uniform S fields. Initially, $\hat{S}$ values vary but quickly stabilize at values that are significantly different from S_{eff}. Again, the solid circle, diamond, triangle, and square symbols connected by lines represent the arithmetically averaged storage coefficient values based on the five different groups of elements surrounding the observation wells. Unlike the $\hat{T}$ values, these $\hat{S}$ values appear to be strongly correlated with the arithmetically averaged values around the observation wells.

3.4. Diagnostic Experiments

[34] To further elucidate the aforementioned results, another experiment was conducted. Figure 8 shows the layout of the new experiment; four distinct blocks (B1 to B4) of different hydraulic properties are embedded in an aquifer of uniform properties. Two scenarios are considered. In case 1 the storage coefficient is assumed to be constant (S = 0.06) for the entire field, including those of the four blocks, while the transmissivity values of the four blocks from B1 to B4 are 0.1, 0.01, 10, and 50 cm^2/s, respectively, and a background transmissivity (T_b) of 1 cm^2/s is used. In case 2 the transmissivity is assumed to be the same for the background and the four blocks (T = 1 cm^2/s); storage coefficients of the four blocks from B1 to B4 are assigned to be 0.006, 0.0006, 0.36, and 0.6, respectively, and the storage coefficient of the background (S_b) is assumed to be 0.06. Here, we use some physically unrealistic values for the properties to underscore the issues we raised earlier. These unrealistic values do not

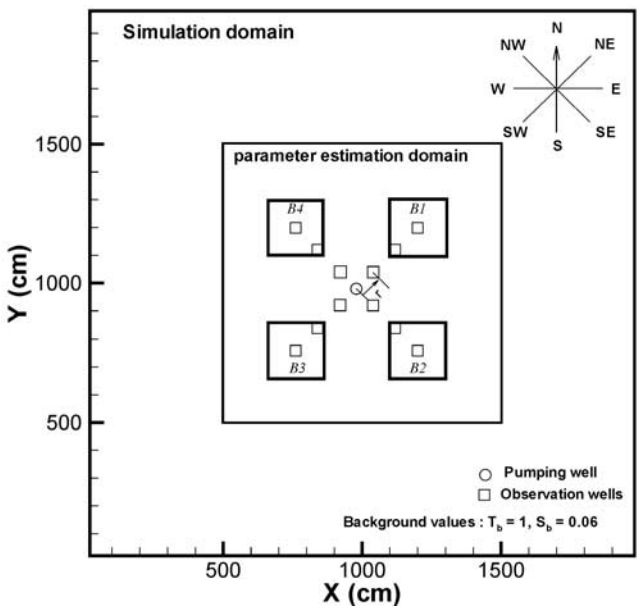

Figure 8. Layout of pumping and observation wells for the diagnostic runs.

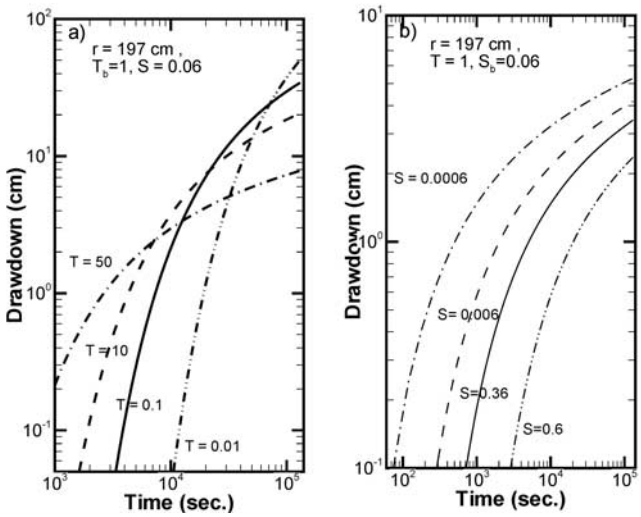

Figure 9. Drawdown time data plots for (a) case 1 and (b) case 2.

invalidate our conclusion. Observation wells are located at r = 85, 197, and 311 cm in the four directions.

[35] The drawdown time curves from the wells located at the center of the four blocks (r = 197 cm) are shown in Figure 9a for case 1. The wells in the blocks with larger T values feel the drawdown earlier and yield greater drawdown than the ones with smaller T values at early time. Behaviors of the drawdown curves are reversed at large time, suggesting large changes in head in low T blocks and thus changes in the flow field at large time due to variation in T. Behaviors of drawdown time curves for case 2 are illustrated in Figure 9b. In this case, the first arrival of the drawdown is observed at the well in the block with the smallest S value. Wells in blocks with large S values feel less drawdown at all time than those in blocks with small values. All the drawdown time curves are parallel over the entire pumping period, indicative of a constant flow pattern. That is, the flow is controlled by the uniform T and not affected by variation in block S values.

[36] These results are relatively easy to explain by considering equation (13) written as:

$$D\nabla^2 h + \frac{Q}{S} = \frac{T}{S}\nabla^2 h + \frac{Q}{S} = \frac{\partial h}{\partial t} \tag{17}$$

Here we drop the subscript *eff* and overhead bar for convenience. In both cases 1 and 2, the first arrival of the drawdown is controlled by D and Q/S (notice that Q is constant). Since S is constant everywhere in case 1, the difference in arrival time is governed by the variation in block T values. In contrast, the difference in case 2 is controlled by the variation in block S values since T is uniform. At large time, the right-hand side of equation (17) is negligible and T therefore is the only controlling factor in both cases. This explains small drawdown in blocks with large T values in case 1 and the parallel drawdown curves in case 2 at large times caused by the uniform T field.

[37] Table 1 summarizes $\hat{T}$ and $\hat{S}$ values at large time and their correlation with T values of blocks in case 1. Values of $\hat{T}$ are fairly constant and close to the background T value and there is no clear correlation between the estimates and the T values of the blocks where the observation well is located. While the values of $\hat{S}$ are close to the value of the entire aquifer, they vary and seemingly are affected by the T value near the observation well, but the relation is unclear. As the observation well is outside the T block (i.e., r = 85), the correlation between the block T values and $\hat{T}$ and $\hat{S}$ values are very high, suggesting $\hat{T}$ and $\hat{S}$ values are influenced by the T block upstream.

Table 1. Case 1: Uniform S (0.06), T Background = 1, and Four Different T Blocks

	$\hat{S}$	$\hat{T}$	T (Block)	Correlation: T (Block) and $\hat{T}$	Correlation: T (Block) and $\hat{S}$
r = 311					
SE	1.4071	0.7703	0.0100	0.4676	0.1940
NE	0.0993	0.5888	0.1000		
SW	0.0536	1.0541	10.0000		
NW	0.0524	1.0515	50.0000		
r = 197					
SE	0.1658	0.5637	0.0100	0.4049	0.0059
NE	0.0687	0.7804	0.1000		
SW	0.1016	1.1101	10.0000		
NW	0.1215	1.0687	50.0000		
r = 85					
SE	0.0543	0.9917	0.0100	0.6240	0.7554
NE	0.0553	1.0034	0.1000		
SW	0.0616	1.1924	10.0000		
NW	0.0646	1.2216	50.0000		

[38] Table 2 tabulates the results of case 2. Values of $\hat{T}$ and $\hat{S}$ are correlated with the block values, when the observation well is at the center of the block (r = 311 cm). As the observation well moves toward the edge of the block (r = 197 cm), the estimated $\hat{S}$ still correlates well with the S value of each block, but to a lesser extent. If the well is completely outside of the block (r = 85), the $\hat{S}$ values are least correlated with the block S values but are close to the background value (S_b = 0.06). These results suggest that the $\hat{S}$ values appear to be an average of S values in between the pumping and the observation wells. Generally, values of $\hat{T}$ are very close to the true value (T = 1); they vary and are influenced by the variation in block S values.

3.5. Cross-Correlation Analysis

[39] Equation (15) is evaluated for given mean values of T and S (T = 0.0035 m^2/s and S = 0.00023), a pumping rate

Table 2. Case 2: Uniform T (1.0), S Background = 0.06, and Four Different S Blocks

	$\hat{T}$	$\hat{S}$	S (Block)	Correlation: $\hat{S}$ and S (Block)	Correlation: $\hat{T}$ and S (Block)
r = 311					
SE	1.5713	0.0441	0.0006	0.9952	0.9241
NE	1.5861	0.0463	0.0060		
SW	0.8273	0.1337	0.3600		
NW	0.7564	0.1774	0.6000		
r = 197					
SE	1.3576	0.0442	0.0006	0.9931	0.9364
NE	1.3738	0.0456	0.0060		
SW	1.0782	0.1076	0.3600		
NW	1.0386	0.1366	0.6000		
r = 85					
SE	1.1789	0.0455	0.0006	0.9367	0.9727
NE	1.1906	0.0455	0.0060		
SW	1.2244	0.0512	0.3600		
NW	1.2442	0.0520	0.6000		

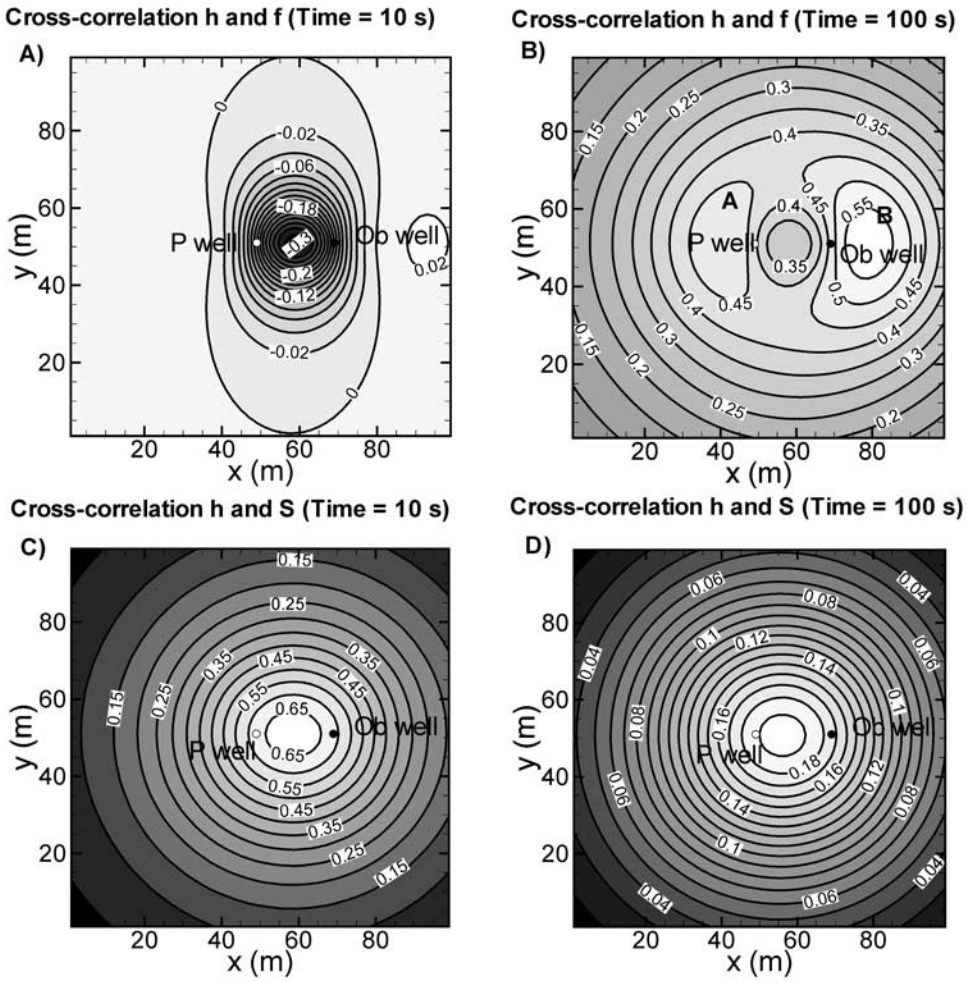

Figure 10. The distributions of the cross-correlations between the observed head and transmissivity field at time = (a) 10 and (b) 100. The distributions of the cross correlations between the observed head and storage coefficient field at time = (c) 10 and (d) 100.

of 0.2m^3/s, and covariance functions of T and S (exponential model with isotropic correlation scales that are 20 m). A constant head of 100 m is assigned to all boundary conditions and the initial head is 100 m everywhere in the domain. Contour maps of the cross correlations between the head at an observation well at a distance (20 m) from the pumping well and T everywhere in the domain (i.e., ρ_{hT}) are plotted in Figures 10a and 10b for early time (t = 10 s) and late time (t = 100 s), respectively. The corresponding maps for the head and the S field are illustrated in Figures 10c and 10d. At early time, the ρ_{hT} values are low everywhere (ranging from 0 to -0.3), with the highest negative correlation (-0.3) located in between the pumping and observation wells (Figure 10a). Meanwhile, the cross correlations between the head and the S field (ρ_{hS}) range from 0.1 to 0.7 at early time. They are much greater than the ρ_{hT} values. Significantly high ρ_{hS} values (>0.65) are confined to the area between the pumping and observation wells (Figure 10c).

[40] Behaviors of the cross-correlation maps reverse at late time, however. Values of ρ_{hT} increase significantly everywhere (ranging from 0.15 to 0.6) covering the entire cone of depression (Figure 10b). Conversely, the ρ_{hS} values decrease, ranging from 0.04 to 0.18 (Figure 10d). The spatial pattern of the ρ_{hS} values remains similar to that at early time. The pattern of the ρ_{hT} values at late time is quite different from that at early time. Highly positive correlations (>0.45) between the head and the T field are limited to two regions (A and B) outside the area between the pumping and the observation well (Figure 10b).

[41] The temporal and spatial distribution of the cross correlations suggest that at early time the head at the observation well mainly reflects the S values in the restricted area between the pumping and observation wells. The head is also weakly and negatively related to the T in the same area. In other words, if the observed head at the observation well is high (or drawdown is small), then the S of the area between the pumping and observation wells is certainly high and the T is possibly low. The strong positive correlation between the head and S is expected because both D and Q/S are controlled by S as shown in equation (17). Conversely, T affects D only. This result corroborates the previous discussion of Figures 9a and 9b. It also explains the findings for case 2 summarized in Table 2: the correspondence between $\hat{S}$ and the S value of each block decreases, and the $\hat{S}$ values approach the background S value as the well moves toward the pumping well and outside the block. The increasing correspondence between

$\hat{T}$ and the S value of each block as the well moves toward the pumping well, seems to suggest that the effect of S heterogeneity is accommodated by $\hat{T}$. More importantly, it provides the reason why $\hat{S}$ values in Figure 7 stabilize to the local values. These local values are likely the average of S values in the restricted area.

[42] Conversely, the observed head at large time is strongly affected by the T values over a large area, in particular the values at the two regions, and has little relation with the S field. This explains the results shown in Figure 6 and case 1 in Table 1. That is, the small differences between $\hat{T}$ values estimated from the four wells at large time are attributed to the fact that the head observed in each block is influenced by the T values over the entire domain. The signature of the T of the blocks borne in $\hat{T}$, on the other hand, is caused by the high ρ_{hT} values in regions A and B (Figure 10b). More precisely, the high ρ_{hT} values behind the observation well explain the increasing correlation (0.624) between $\hat{T}$ and the block T value as the observation moves toward the pumping well and outside the block.

4. Discussion

[43] Our new approaches for estimating the effective T of an aquifer with multilog Gaussian T and S fields yield the same results as many previous studies: it is a geometric mean. On the other hand, the effective S of an aquifer is its arithmetic mean. These approaches and the finding regarding the effective S are new.

[44] A cross-correlation analysis has also been developed that yields insight to the meaning of the estimated T and S from the traditional analysis of aquifer tests. That is, the $\hat{S}$ value obtained from the traditional Theis analysis likely represents a weighted average of S values mainly over the region between the pumping and observation wells. This is an important finding since the storage coefficient is the parameter for evaluating groundwater reserves in a basin. It represents the amount of groundwater released from a unit area of an aquifer per head drop. As an aquifer encompasses a large area, an incorrect estimate of S can yield a gross underestimate or overestimate of groundwater availability of the aquifer. Therefore knowing the true meanings of the estimate of S from the aquifer test is of critical importance to groundwater resource management. Further, the narrow region of high cross correlation between the head and S fields explains large variability of S estimates from the traditional analysis of aquifer tests, as reported by previous investigators.

[45] In contrast to the $\hat{S}$ value, the $\hat{T}$ value is a weighted average of all T values in the entire domain. This finding appears to support the inverse radial distance averaging rule by *Desbarats* [1992] for effective transmissivity. Comparing with those of S, the weights associated with T are higher over the entire aquifer, in particular near regions A and B. Relatively high weights over the entire aquifer imply that $\hat{T}$ can also be influenced by any large-size or strong anomaly (e.g., boundaries, faults, etc.) within the cone of depression. Thus an interpretation of the meaning of $\hat{T}$ can be highly uncertain and in turn, our previous assessments of variability of transmissivity of aquifers may be subject to serious doubt. In the Gaussian random medium examined in the study, $\hat{T}$ is close to the geometric mean but does not equal the geometric mean, and is instead influenced by local values (regions A and B in Figure 10b).

[46] The time-varying spatial variances of the drawdown (Figure 5) also challenge the traditional analysis of anisotropy of the effective transmissivity of aquifers. Traditional analysis of transmissivity anisotropy uses three observation wells and one pumping well [*Papadopulos*, 1965] or three wells with alternate pumping locations [*Neuman et al.*, 1983]. According to the drawdown distribution in Figure 2 and the spatial variances in Figure 5, it is evident that even though the aquifer is statistically isotropic, yielding behaviors similar to those in homogeneous aquifers with large-scale anisotropy, the shapes of the cone of depressions are highly irregular and influenced by local heterogeneity. Further, the principal directions of the elliptic cone of depression change with time as the depression evolves. Accordingly, a salient question to be asked is: Would drawdown collected at a few wells be sufficient to capture the general shape of the cone of depression? Also: How long does an aquifer test have to last such that a stable shape of the cone of depression can be captured if it does stabilize?

[47] Last, our analyses are built upon a 2-D flow model with horizontally varying T and S. Undoubtedly, analysis using 3-D models that consider both horizontal and vertical heterogeneity of aquifers at a multiplicity of scales is most appropriate. In addition, our cross-correlation analysis is a first-order approximation. Therefore our analysis is not impeccable but certainly casts serious doubts about the validity of traditional aquifer analyses that use drawdown time data from a limited number of observation wells. Theis' analysis has unequivocally played a significant role in advancing the subsurface hydrologic sciences, but its validity needs to be questioned when it is applied to a real-world problem, where aquifers are inherently heterogeneous. Likewise, the study of slug tests by *Beckie and Harvey* [2002] also indicated that while slug tests are useful to estimate transmissivities, they yield dubious values for storage coefficients. Recently developed tomographic surveys [e.g., *Gottlieb and Dietrich*, 1995; *Vasco and Datta-Gupta*, 1999; *Yeh and Liu*, 2000; *Vesselinov et al.*, 2001; *Meier et al.*, 2001; *Liu et al.*, 2002; *Bohling et al.*, 2002; *Brauchler et al.*, 2003; *McDermott et al.*, 2003; *Zhu and Yeh*, 2005] seem to be the increasingly preferred methods for aquifer tests, in particular, hydraulic tomography. Although most of the hydraulic tomography analyses have been demonstrated for vertical heterogeneity, hydraulic tomography can unequivocally be applied to 2-D depth-averaged aquifer analysis. For example, if several wells are available in an area, a pumping test can be conducted at one of the wells and hydrographs can be recorded at the others. Afterward, pumping can be initiated at a different well and at the other wells drawdown is recorded, and this process is repeated for the other wells. Such a sequential cross-well interference test provides more data sets using existing well facilities than the traditional aquifer test can. Subsequently, appropriate inverse modeling [e.g., *Yeh et al.*, 1996; *Yeh and Liu*, 2000; *Zhu and Yeh*, 2005] of these data sets can yield an estimate of the 2-D heterogeneity pattern in the area, which is more accurate and useful than hydraulic properties estimated from the traditional aquifer test and analysis using

the same well facilities. A program for interpreting a 2-D hydraulic tomography survey is available at http://www.hwr.arizona.edu/yeh/download/.

5. Summary and Conclusions

[48] We present two estimation approaches (i.e., distance drawdown and spatial moment analyses) for S_{eff} and T_{eff}, which are consistent with Theis' homogeneous aquifer assumption. We find that (1) S_{eff} and T_{eff} values evolve with time, as well as the principal directions of the transmissivity, (2) S_{eff} approaches the arithmetical mean of the field, (3) T_{eff} converges to its geometric mean at large time for the Gaussian random field we generated, and (4) the averages of local T and S values within the cone of depression at early times differ from the T_{eff} and S_{eff} values. Both the averages and effective parameters, however, agree at large times, indicative of the existence of an REV in our domain if the pumping time is sufficiently long and there are no other effects (such as boundaries).

[49] Our numerical experiments and cross-correlation analysis of $\hat{T}$ and $\hat{S}$ estimates from drawdown time data at a single observation well, induced by a pumping well, lead to the following findings. At early time, estimated $\hat{T}$ and $\hat{S}$ values change with time, deviating significantly from the geometric means of the fields. The $\hat{S}$ values stabilize rather quickly at the value dominated by the geology between the pumping and the observation well. At late times, values of $\hat{T}$ approach but do not equal the geometric mean, and are influenced by the location, size, and degree of heterogeneity as the cone of depression evolves.

[50] Last, we conclude that, because of the inherent heterogeneity of aquifers, traditional analyses of aquifer tests that fit the drawdown time data to the Theis-type curve or Jacob's approximate solution may yield estimates of the transmissivity and storage coefficient that are difficult to interpret. Only if sufficiently long pumping is conducted does the estimated transmissivity become close to, but still not equal to, some mean of the aquifer. In contrast, the estimated S is dominated by the local average S between the pumping and observation wells. These findings are of great importance for water resources development and management, in addition to water quality protection. A new generation of aquifer test technologies, such as hydraulic tomography [*Yeh and Liu*, 2000; *Liu et al.*, 2002; *Zhu and Yeh*, 2005], must be developed and applied to field problems.

[51] **Acknowledgments.** This study was a part of activities of the first author during his visit at the Department of Hydrology and Water Resources at the University of Arizona. The first author acknowledges the financial support from the GSSAP Program (NSC 93-2917-I-002-020) of the National Science Council of Taiwan. Many thanks also are extended to the Department of Hydrology and Water Resources for providing an enjoyable working environment for the first author. The research was also partially supported by NSF/SERDP grant EAR 0229717 and NSF SIIE grant IIS-0431079. Many thanks are extended to Alexandre Desbarats for his insightful and constructive review on our revised manuscript. Our gratitude is also extended to Martha P.L. Whitaker for technical editing of the manuscript. Finally, we are in debt to the two anonymous reviewers and the AE who have spent enormous efforts reviewing the manuscript and provided very encouraging, insightful, and constructive comments.

References

Aris, R. (1956), On the dispersion of a solute in a fluid flowing through a tube, *Proc. R. Soc. London, Ser. A*, *235*, 67–78.

Bear, J. (1988), *Dynamics of Fluids in Porous Media*, 764 pp., Dover, Mineola, N. Y.

Beckie, R., and C. F. Harvey (2002), What does a slug test measure: An investigation of instrument response and the effects of heterogeneity, *Water Resour. Res.*, *38*(12), 1290, doi:10.1029/2001WR001072.

Bohling, G. C., X. Zhan, J. J. Butler Jr., and L. Zheng (2002), Steady-shape analysis of tomographic pumping tests for characterization of aquifer heterogeneities, *Water Resour. Res.*, *38*(12), 1324, doi:10.1029/2001WR001176.

Bosch, D. D., and T.-C. J. Yeh (1989), Effective unsaturated hydraulic conductivity for computing one-dimensional flow in heterogeneous porous media, *Trans. ASAE*, *32*(6), 2035–2040.

Brauchler, R., R. Liedl, and P. Dietrich (2003), A travel time based hydraulic tomographic approach, *Water Resour. Res.*, *39*(12), 1370, doi:10.1029/2003WR002262.

Butler, J. J., Jr., and W. Liu (1993), Pumping tests in non-uniform aquifers: The radially asymmetric case, *Water Resour. Res.*, *29*(2), 259–269.

Chrysikopoulos, C. V. (1995), Effective parameters for flow in saturated heterogeneous porous media, *J. Hydrol.*, *170*, 181–197.

Cooper, H. H., Jr., and C. E. Jacob (1946), A generalized graphical method for evaluating formation constants and summarizing well-field history, *Eos Trans. AGU*, *27*(4), 526–534.

de Marsily, G. (1986), *Quantitative Hydrogeology: Groundwater Hydrology for Engineers*, 440 pp., Elsevier, New York.

Desbarats, A. J. (1992), Spatial averaging of transmissivity in heterogeneous fields with flow towards a well, *Water Resour. Res.*, *28*(3), 757–767.

Fisher, H. B., E. J. List, R. C. Y. Koh, J. Imberger, and N. H. Brooks (1979), *Mixing in Inland and Coastal Waters*, 483 pp., Elsevier, New York.

Gottlieb, J., and P. Dietrich (1995), Identification of the permeability distribution in soil by hydraulic tomography, *Inverse Probl.*, *11*, 353–360.

Gutjahr, A. L. (1989), Fast Fourier transforms for random field generation, project report for Los Alamos grant, contract 4-R58-2690R, Dep. of Math., N. M. Tech., Socorro.

Hughson, D. L., and T.-C. J. Yeh (2000), An inverse model for three-dimensional flow in variably saturated porous media, *Water Resour. Res.*, *36*(4), 829–839.

Indelman, P. (2003), Transient pumping well flow in weakly heterogeneous formations, *Water Resour. Res.*, *39*(10), 1287, doi:10.1029/2003WR002036.

Jonse, L. D., T. Lemar, and C. T. Tsai (1992), Results of two pumping tests in Wisconsin age weathered till in Iowa, *Ground Water*, *30*(4), 529–538.

Li, B., and T.-C. J. Yeh (1998), Sensitivity and moment analyses of head in variably saturated regimes, *Adv. Water Resour.*, *21*(6), 477–485.

Liu, S., T.-C. J. Yeh, and R. Gardiner (2002), Effectiveness of hydraulic tomography: Sandbox experiments, *Water Resour. Res.*, *38*(4), 1034, doi:10.1029/2001WR000338.

McDermott, C. I., M. Sauter, and R. Liedl (2003), New experimental techniques for pneumatic tomographical determination of the flow and transport parameters of highly fractured porous rock samples, *J. Hydrol.*, *278*(1–4), 51–63.

Meier, P. M., J. Carrera, and X. Sanchez-Vila (1998), An evaluation of Jacob's method for interpretation of pumping tests in heterogeneous formations, *Water Resour. Res.*, *34*(5), 1011–1025.

Meier, P. M., A. Median, and J. Carrera (2001), Geostatistical inversion of cross-hole pumping tests for identifying preferential flow channels within a shear zone, *Ground Water*, *39*(1), 10–17.

Neuman, S. P., G. R. Walter, H. W. Bentley, J. J. Ward, and D. D. Gonzalez (1983), Determination of horizontal aquifer anisotropy with three wells, *Ground Water*, *22*(1), 66–72.

Oliver, D. (1993), The influence of nonuniform transmissivity and storativity on drawdown, *Water Resour. Res.*, *29*(1), 169–178.

Papadopulos, I. S. (1965), Nonsteady flow to a well in an infinite anisotropic aquifer, in *Proceedings of Dubrovnik Symposium on the Hydrology of Fractured Rocks*, *IASH Publ.*, *73*, 12–31.

Sánchez-Vila, X., P. M. Meier, and J. Carrera (1999), Pumping test in heterogeneous aquifers: An analytical study of what can be obtained from their interpretation using Jacob's method, *Water Resour. Res.*, *35*(4), 943–952.

Sykes, J. F., J. L. Wilson, and R. W. Andrews (1985), Sensitivity analysis for steady state groundwater flow using adjoint operators, *Water Resour. Res.*, *21*(3), 359–371.

Taylor, G. I. (1921), Diffusion by continuous movements, *Proc. London Math. Soc., Ser. A*, *20*, 196–211.

Theis, C. V. (1935), The relation between lowering the piezometric surface and the rate and duration of discharge of a well using ground water storage, *Eos Trans. AGU*, *16*, 519–524.

Vasco, D. W., and A. Datta-Gupta (1999), Asymptotic solutions for solute transport: A formalism for tracer tomography, *Water Resour. Res.*, *35*(1), 1–16.

Vesselinov, V. V., S. P. Neuman, and W. A. Illman (2001), Three-dimensional numerical inversion of pneumatic cross-hole tests in unsaturated fractured tuff: 2. Equivalent parameters, high-resolution stochastic imaging and scale effects, *Water Resour. Res.*, *37*(12), 3019–3042.

Walton, W. G. (1970), *Groundwater Resource Evaluation*, 663 pp., McGraw-Hill, New York.

Ye, M., R. Khaleel, and T.-C. J. Yeh (2005), Stochastic analysis of moisture plume dynamics of a field injection experiment, *Water Resour. Res.*, *41*, W03013, doi:10.1029/2004WR003735.

Yeh, T.-C. J. (1989), One-dimensional steady-state infiltration in heterogeneous soils, *Water Resour. Res.*, *25*(10), 2149–2158.

Yeh, T.-C. J. (1998), Scale issues of heterogeneity in vadose-zone hydrology, in *Scale Dependence and Scale Invariance in Hydrology*, edited by G. Sposito, pp. 224–265, Cambridge Univ. Press, New York.

Yeh, T.-C. J., and S. Liu (2000), Hydraulic tomography: Development of a new aquifer test method, *Water Resour. Res.*, *36*(8), 2095–2105.

Yeh, T.-C. J., R. Srivastava, A. Guzman, and T. Harter (1993), A numerical model for water flow and chemical transport in variably saturated porous media, *Ground Water*, *31*(4), 634–644.

Yeh, T.-C. J., M. Jin, and S. Hanna (1996), An iterative stochastic inverse approach: Conditional effective transmissivity and head fields, *Water Resour. Res.*, *32*(1), 85–92.

Yeh, T.-C. J., M. Ye, and R. Khaleel (2005), Estimation of effective unsaturated hydraulic conductivity tensor using spatial moment of observed moisture plumes, *Water Resour. Res.*, *41*, W03014, doi:10.1029/2004WR003736.

Zhu, J., and T. J. Yeh (2005), Characterization of aquifer heterogeneity using transient hydraulic tomography, *Water Resour. Res.*, *41*, W07028, doi:10.1029/2004WR003790.

C.-H. Chen, Department of Civil Engineering, ChungKuo Institute of Technology, Taipei 106, Taiwan.

N.-S. Hsu, T. H. Lee, and C.-M. Wu, Department of Civil Engineering, National Taiwan University, Taipei 106, Taiwan.

A. F. Sancho, Unitat de Geodinàmica Externa i Hidrogeologia, Departamento de Geologia, Universitat Autònoma de Barcelona, E-08193, Bellaterra, Spain.

T.-C. J. Yeh and J. Zhu, Department of Hydrology and Water Resources, University of Arizona, Tucson, AZ 85721, USA. (ybiem@mac.hwr.arizona.edu)